DETAILED STUDY ON THE PASSIVATION MECHANISM OF a-Si_xC_{1-x} FOR THE SOLAR CELL REAR SIDE

D. Suwito[1], T. Roth[1], D. Pysch[1], L. Korte[2], A. Richter[1], S. Janz[1], S. W. Glunz[1]

[1]Fraunhofer Institute for Solar Energy Systems ISE, Heidenhofstr. 2, D-79110 Freiburg
[2] Helmholtz-Zentrum Berlin für Materialien und Energie, Kekuléstrasse 5, D-12489 Berlin
Corresponding author: Dominik Suwito, Tel.: +49-761-4588-5435, Fax.: +49-761-4588-9250,
E-mail: dominik.suwito@ise.fraunhofer.de

ABSTRACT: In this work we focus on the surface passivation of *p*-FZ, 1 Ωcm silicon wafers by intrinsic, silicon-rich, amorphous silicon carbide (a-Si_xC_{1-x}:H) with excellent passivation quality (S_{eff} < 5 cms^{-1} for *p*- and *n*-type 1 Ωcm silicon at Δn=5·10^{14} cm^{-3}). For the purpose of extracting the effective surface recombination velocity (S_{eff}) independent of the bulk properties, we use a set of identically passivated wafers of different substrate thickness (W). The injection-dependent carrier lifetime $\tau_{eff}(\Delta n)$ is determined in a wide injection level range (10^{10}-10^{17} cm^{-3}) using a combination of the quasi-steady-state photoconductance (QSS-PC) and photoluminescence (QSS-PL) technique. S_{eff} is extracted by evaluation of the slope of the $1/\tau_{eff}$ vs. $1/W$ plot for each injection level without any additional assumptions on the bulk lifetime. These pure S_{eff} data obtained in such a way is then used within the simple Shockley-Read-Hall (SRH) model to extract surface parameters such as the interface charge density Q_f. Surface photovoltage measurements (SPV) performed on the a-SiC/c-Si system confirm an amphoteric behaviour of the interface charge. Our study shows that the low-injection lifetime data determined by QSS-PL plays a crucial role for the accurate modelling of surface parameters.

Keywords: c-Si, passivation, a-SiC

1 INTRODUCTION

The plasma-enhanced chemical vapour deposition (PECVD) technique allows the low temperature fabrication of passivating layers for the crystalline silicon surface. The most widespread and studied representatives in photovoltaics are certainly SiN_x and a-Si. The former constitutes the standard passivation scheme for the front side of industrial solar cells as the tunability of its optical parameters is useful for the optimisation of anti-reflection properties. However, the use of SiN_x for the passivation of the rear side of *p*-type silicon solar cells is unfavourable due to the high fixed charge density in the material and the resulting decrease in passivation quality when being contacted [1]. a-Si passivation exhibits very low surface recombination velocities [2], but has clear disadvantages when it comes to the point of thermal stability and degradation effects. A main field of application for a-Si layers are hetero-junction solar cells as the latter require essentially low interface state densities and the dopability of the amorphous network [3]. As compared to a-Si, a-Si_xC_{1-x}:H possesses an additional degree of freedom owing to the tunable amount of carbon in the network. Although Si-rich layers are clearly superior to their C-rich counterparts in terms of passivation quality, there exists a certain ratio of silicon to carbon atoms for which the surface recombination is minimised [4]. An elevated thermal stability of a-Si_xC_{1-x}:H [5] presents a major difference to single layer a-Si passivation and, as in the case of SiN_x, the stoichiometry of the network allows engineering of its optical parameters [6].

In this work we aim at clarifying the role of the field effect passivation through fixed charges at the interface in excellently passivating, Si-rich a-Si_xC_{1-x}:H films. The field-effect is undesirable since it might involve performance losses when used in rear passivation schemes for solar cells [1].

2 EXPERIMENTAL DETAILS

2.1 Sample preparation

Boron doped float-zone (FZ) silicon wafers with <100> surface orientation and 1 Ωcm resistivity were used in this study. The samples were mechanically thinned using a grinder [7]. The thinning was followed by a short KOH etch in order to remove the surface damage. The resulting thickness variation of the wafers is displayed in Table I. The pre-treatment of the wafer surfaces consisted of a RCA clean on the day before the deposition of the passivation layer. The a-Si_xC_{1-x}:H layers were deposited by PECVD in an AK400M reactor from Roth&Rau using silane (SiH_4) and methane (CH_4) as precursor gases and low power densities provided by a high frequency (13.65 MHz) generator. 35 nm of a-Si_xC_{1-x}:H were grown on both sides of the wafers at a temperature of 300-350°C.

Table I Thickness after grinding and KOH etch of the p-FZ, 1 Ωcm wafers used in this study.

Thickness (μm)				
193	119	84	53	44

2.2 Lifetime measurement

The effective excess carrier lifetime of the passivated samples in the injection regime 10^{14}-10^{17} cm^{-3} was determined with a WCT-120 Photoconductance Tool from Sinton Consulting Inc. in the transient and quasi steady state (QSS-PC) mode [8]. The low injection lifetimes (Δn=10^{10}-10^{14} cm^{-3}) were accessed by the QSS-PL technique [9] using the same setup as described in [10]. For each wafer the QSS-PL was calibrated self-consistently [11] resulting in a perfect match of the PL and PC data.

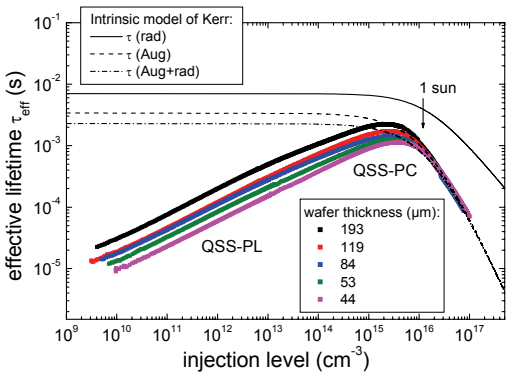

Figure 1 Injection dependent effective lifetimes determined by the QSS-PC and -PL technique. There is a perfect match between the data of the two caracterization methods. The measured excellent lifetimes seem to conflict with the intrinsic recombination model.

2.3 Discussion of the lifetime data

The measured lifetime data show an overall excellent passivation quality of intrinsic a-Si_xC_{1-x}:H with a quasi linear decrease to lower injection levels (Figure 1). In the range of 10^{15}-10^{16} cm^{-3}, the lifetimes of all samples approach the intrinsic limit of the Si-bulk, that is the limit due to radiative and Auger recombination, and apparently "surpass" this limit in the case of the 193 and 119 µm thick sample. The intrinsic limitations depicted in Figure 1 are based on the model of Kerr and Cuevas [12] who basically evaluated the highest lifetime data available for the accurate parameterization of band-to-band Auger recombination. While the data for the Auger recombination alone (dashed line) are exceeded only to a small amount, the discrepancy for the model including Auger and radiative recombination (dash-dotted line) is significant. The coefficient for the radiative recombination assumed throughout their approach is the rather high value proposed by Schlangenotto *et al.* of B=9.5·10^{-15} cm^3s^{-1} [13] and therefore exhibits a rather high impact on the total intrinsic recombination limit. Our measurements seem to be reliable and we believe that there are no measurement uncertainties that could account for a 40% error in the determined data. However, a more precise analysis regarding the discrepancy between our measured lifetimes and the model still has to follow up.

3 EXTRACTION OF S_{eff}

The prepared set of lifetime samples allows two different approaches to extracting the effective recombination velocity (S_{eff}) from the measured lifetimes. Both methods are based on the equation

$$\frac{1}{\tau_{eff}} = \frac{1}{\tau_{bulk}} + \frac{2S_{eff}}{W}, \qquad (1)$$

which holds for sufficiently small values of S_{eff} [14]. W denotes the wafer thickness and τ_{bulk} is related to the radiative (τ_{rad}), Auger (τ_{Aug}) and Shockley-Read-Hall (τ_{SRH}) lifetime via

$$\frac{1}{\tau_{bulk}} = \frac{1}{\tau_{Aug}} + \frac{1}{\tau_{rad}} + \frac{1}{\tau_{SRH}} \cdot \qquad (2)$$

3.1 S_{eff} via assumptions concerning τ_{bulk}

If τ_{bulk} is known, S_{eff} can be calculated directly from equation (2) for each wafer. As the most difficultly accessible parameter is τ_{SRH} and as recombination via defects in float-zone silicon is supposed to be negligible, the most common approximation is the mere consideration of the intrinsic recombination limits through an adequate model (throughout this work we use the Kerr parameterization). The injection dependent S_{eff} values for three exemplary samples extracted in this way are shown in Figure 3 and Figure 4.

3.2 Extraction of S_{eff} by thickness variation of substrates

The second method makes use of equally passivated samples of different thickness W. The injection dependent S_{eff} can be extracted from the slope of a $1/\tau_{eff}$ vs. $1/W$ plot (Figure 2) [7]. Note that no additional assumptions have to be made concerning the bulk lifetime. The S_{eff} values determined in this way, including the error bars resulting from the uncertainty of the linear regression of the corresponding τ_{eff} data, are plotted in Figure 3 and Figure 4 (black squares).

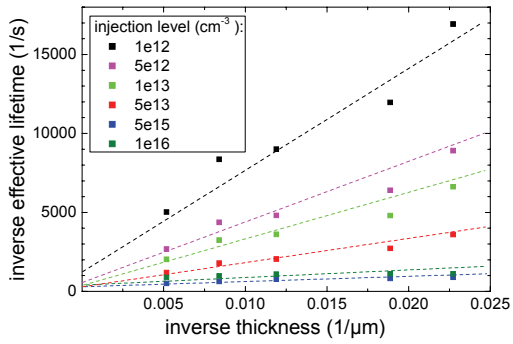

Figure 2 Inverse effective lifetimes vs. inverse thickness for different injection densities. The slope of the fitted line corresponds to $2S_{eff}$.

3.3 Discussion of the S_{eff} data

As already pointed out, all extracted S_{eff} curves indicate a quasi-linear injection dependence, that is, linearly increasing surface recombination velocities towards lower injection regimes. The log-log graph (Figure 3) reveals the difference between the differently determined S_{eff} values at high injection levels (>10^{14} cm^{-3}): In this range the intrinsic recombination processes are dominant and due to the above mentioned conflict of our very high lifetime data with the model, S_{eff} becomes very small and even negative for method 1. The "pure" S_{eff} data obtained by method 2 are independent of the intrinsic lifetime model and show a transition to constant or even increasing surface recombination velocities when the injection density approaches the dopant density (1.5·10^{16} cm^{-3}).

The semi-logarithmic graph in Figure 4 depicts the difference of the two methods in the low injection regime. As expected, the S_{eff} data determined by method 1

exhibit an upper limit for the "real" values. Figure 4 also confirms, that the accuracy of method 1 decreases with increasing wafer thickness, since the assumption of a perfect crystal ($\tau_{SRH} \rightarrow \infty$) becomes more and more inappropriate for an increasing volume to surface ratio.

These results indicate, that the extraction of the surface recombination velocity under high injection by method 1 is fundamentally affected by the chosen intrinsic lifetime model, the more severe the higher the lifetimes of the samples are. In the low injection regime the inaccuracy of method 1 stems from the SRH recombination in the bulk. As can be concluded from the comparison of the "pure" and approximated S_{eff} data, SRH recombination in the bulk becomes more pronounced for lower injection densities.

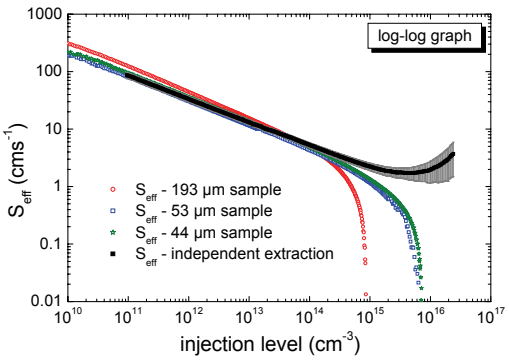

Figure 3 Log-log graph of the injection-dependent effective recombination velocity (S_{eff}). The black squares with gray error bars represent S_{eff} extracted via the thickness variation method for the set of samples under consideration. The red circles, blue squares and the green stars refer to S_{eff} of the 193, 53 and 44 µm thick samples, respectively, assuming a bulk lifetime only limited by intrinsic recombination processes.

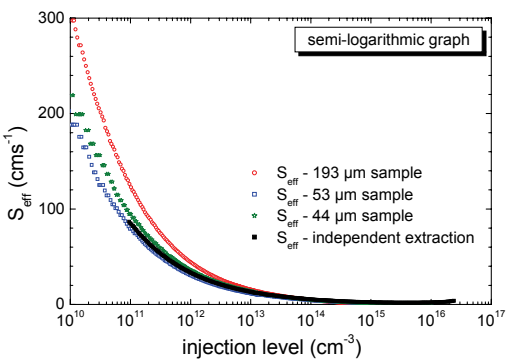

Figure 4 Semi-logarithmic graph of the injection-dependent effective recombination velocity (S_{eff}). The black squares represent S_{eff} extracted via the thickness variation method for the set of samples under consideration (error bars omitted for clarity). The red circles, blue squares and the green stars refer to S_{eff} of the 193, 53 and 44 µm thick samples, respectively, assuming a bulk lifetime only limited by intrinsic recombination processes.

4 MODELING

For the extraction of surface parameters from the injection-dependent surface recombination velocities we make use of the so-called "extended Shockley-Read-Hall formalism" and a numerical algorithm proposed by Girisch *et. al* [15]. This model was designed for the description of interface parameters of metal-oxide-semiconductor (MOS) systems and therefore assumes a perfect insulator in contact with the silicon surface. Although intrinsic a-Si_xC_{1-x}:H can be considered as a low band-gap insulator (E_g=1.7-1.9 eV), the disregard of an additional recombination path for minority carriers of the crystal in the a-Si_xC_{1-x}:H bulk and "hetero" effects like the band offsets at the interface constitute a considerable simplification of our real system. Moreover, we merely consider one active recombination centre in the band-gap situated at the intrinsic energy E_i and no recombination in the space charge region at the c-Si surface. Neglecting any injection dependence of the fixed charges in the passivation layer, the model parameters are reduced to the fixed charge density Q_f and the fundamental recombination velocities S_{n0} and S_{p0} with

$$S_{n0/p0} = v_{th} N_{st} \sigma_{n/p}, \qquad (3)$$

v_{th} is the thermal velocity of the charge carriers and N_{st} denotes the density of defects per unit of area. The relation between the surface recombination velocity S_{eff} and the model parameters is given through the Shockley-Read-Hall theory

$$U_S = S_{eff} \cdot \Delta n_S = \frac{n_S p_S - n_i^2}{\frac{n_S + n_i}{S_{p0}} + \frac{p_S + n_i}{S_{n0}}}, \qquad (4)$$

where n_S and p_S are directly related to Q_f through the surface banding ψ_s.

Figure 5 shows the result of a fit of the modelled (red dots) to the extracted (black line) S_{eff} data, assuming a ratio of $S_{n0}/S_{p0} \approx 100$, which is a common assumption for the SiO_2-Si interface [16]. It has to be mentioned that the consideration of three free parameters (Q_f and S_{n0}, S_{p0}) does not lead to a fundamental improvement of the fit quality, but results in an extreemly assymmetric and therefore non-physical ratio of the fundamental recombination velocities. The calculated S_{eff} data through the SRH model agrees merely roughly with the extracted data. This discrepancy can be addressed to the above mentioned over-simplification of our model. The determined fixed charge density Q_f=2.1·10^{11} cm^{-3} allows to describe the major trend of our data of the injection dependent S_{eff}, but fails in modelling the linearity of S_{eff} in the low and mid injection range.

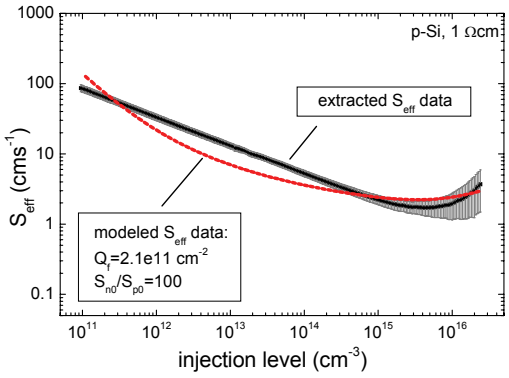

Figure 5 Best fit (red dots) of the simplified SRH-model to the pure injection dependent S_{eff} data (black line) assuming S_{n0}/S_{p0}=100.

5 DISCUSSION OF THE FIXED CHARGE DENSITY

Figure 6 shows the injection dependent S_{eff} values extracted via method 1 for an a-Si_xC_{1-x}:H passivated *n*-type float-zone silicon wafer of 1 Ωcm resistivity (black line). The measured very high lifetimes of the sample again conflict with the intrinsic recombination model and result in a strong decrease in S_{eff} for $\Delta n>10^{15}$ cm^{-3} (black, open circles). The injection dependence of S_{eff} on *n*-type substrate reveals the same characteristics as the one on their *p*-type counterparts, that is the linearity for low and mid injection densities. Emanating from a behaviour similar to that of the SiO_2-Si interface, we would expect a similar set of model parameters as the ones used for *p*-type silicon to be appropriate for the description of the *n*-type counterpart. However, the parameters displayed in Figure 5 applied on *n*-type silcon results in a absolutely different injection trend of S_{eff} represented by the red doted line in Figure 6.

The apparent disagreement between the measured and modelled data for *n*-type substrate is clarified by the measurement of the surface potential ψ_s of the a-SiC/c-Si sytem by means of the surface photovoltage technique (SPV) [17]. Making the simplifications pointed out above, ψ_s is directly related to the fixed charge density Q_f in our model (see Figure 7 and Figure 8). The outcome of the measurements not only suggests that the values of Q_f vary depending on the substrate doping, but that there is even a change of sign for the surface band bending, therefore indicating a negative fixed charge density at the a-SiC/c-Si interface for *n*-type silicon (Table II).

Table II Determined surface band bending at the a-SiC/c-Si interface.

	p-Si, 1 Ωcm	*n-Si, 1 Ωcm*
surface photovoltage measurements	0.41 V	-0.16 V

Maintaining the ratio S_{n0}/S_{p0}=100 and considering the negative value of $Q_f \approx -1.0 \cdot 10^{11}$ cm^{-2} corresponding to the measured ψ_s, we obtain modelled S_{eff} that reproduce the measured increasing recombination towards lower injection densities correctly. However, as is the case for *p*-type substrate, the linear dependence of S_{eff} on the injection level cannot be described by our simple model.

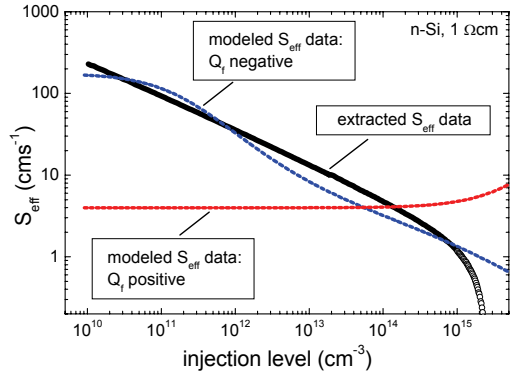

Figure 6 Injection-dependent effective surface recombination velocities for a-Si_xC_{1-x}:H passivated *n*-type float-zone silicon of 1 Ωcm resistivity determined by method 1 (black line). The red doted line corresponds to the modelled S_{eff} values assuming the fit parameters for the *p*-type substrate. Considering negative Q_f values yields the blue doted line.

Our simplified surface model cannot distinguish between fixed charges in the a-Si_xC_{1-x}:H bulk and charges at the interface. The model parameter Q_f therefore has to be interpreted as an effective fixed charge density situated at the a-SiC/c-Si interface. The change of sign of this charge depending on the doping of the substrate was already observed by Martín [18]. Olibet *et. al* encounter the same phenomenon at the a-Si:H/c-Si interface and introduce a model for the description of the surface recombination mechanism based on these amphoteric defects that are attributed to silicon dangling bonds [19]. The basic difference between the latter and the SRH model used in this study consists of the consideration of three (positive, neutral and negative) instead of two (neutral and negative) charge conditions of a discrete recombination level. The consequence are four possible capture events resulting in two parallel recombination paths. Therefore, the model based on amphoteric dangling bonds at the interface provides two additional degrees of freedom, i.e. two additional capture cross sections.

We conclude that for a more quantitative analysis of the effective recombination velocity at the a-SiC/c-Si interface in the future, our surface model has to be extended considering the in this work verified amphoteric behaviour of the fixed charge density.

6 PASSIVATION MECHANISM

Considering the rear side passivation of *p*-type silicon solar cells by Si-rich, intrinsic a-Si_xC_{1-x}:H, Figure 7 indicates that for the case of non-injection (in the dark) the rear surface is just at the onset of inversion (electron density n_s > hole density p_s). However, for the relevant case of illumination, corresponding to injection densities between 10^{14} and 10^{16} cm^{-3} (blue and red line respectively), the surface band bending decreases drastically and the ratio n_s/p_s therefore tends towards one.

Similar considerations hold for *n*-type substrates (Figure 8). Of course this general trend holds for all passivation schemes. However, comparing the measured band bending at the a-SiC/c-Si interface to the induced band banding of SiN_x passivated p-Si, 1 Ωcm surfaces (a typical Q_f of 10^{12} cm^{-2} for SiN_x [20] corresponds to a ψ_s of about 0.82 V), we conclude that the classical field-effect passivation is of considerably lower relevance for the passivation quality of a-Si_xC_{1-x}:H layers as compared to their SiN_x counterparts.

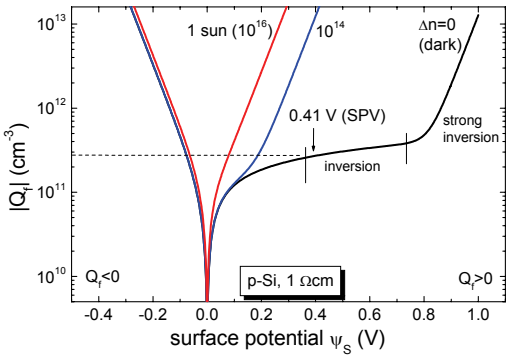

Figure 7 Interrelation of the surface potential ψ_s and the effective fixed charge density at the a-SiC/c-Si interface for, 1 Ωcm silicon. Displayed is the surface band bending for the injection densities 0 (black line), 10^{14} (blue line) and 10^{16} cm^{-3} (red line).

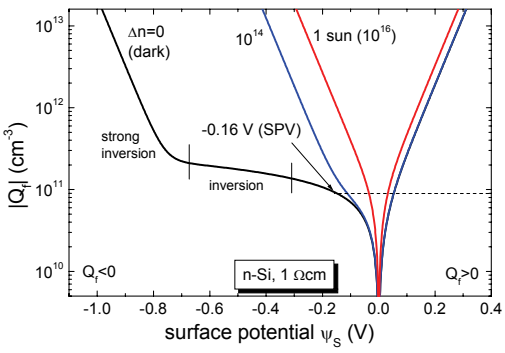

Figure 8 Interrelation of the surface potential ψ_s and the effective fixed charge density at the a-SiC/c-Si interface for *n*-type, 1 Ωcm silicon. Displayed is the surface band bending for the injection densities 0 (black line), 10^{14} (blue line) and 10^{16} cm^{-3} (red line).

Our measurements of the surface potential of a-Si/c-Si interfaces in contrast reveal similar fixed charge densities as for the a-SiC/c-Si interface. This suggests, that the passivation mechanism of Si-rich a-Si_xC_{1-x}:H, analogously to a-Si, can predominantly be addressed to an effective saturation of interface dangling bonds.

7 SUMMARY

For a set of a-Si_xC_{1-x}:H passivated samples with very high carrier lifetimes, we extracted the injection dependent S_{eff} values in two different ways. The first one is the common way of assuming negligible SRH recombination in the bulk and considering radiative and Auger recombination through theoretical or empirical models. The second method is exclusively based on the evaluation of equally passivated samples with varying thickness, hence providing "pure" S_{eff} data. A comparison of the extracted data in a large injection range shows that for method 1 there exists a major dependence on the chosen intrinsic recombination model in the high injection regime and an apparent error for low injection densities due to SRH recombination in the bulk.

For a subsequent modelling of the S_{eff} data, the wide injection range accessible through the combination of the two characterisation techniques QSS-PL and -PC provides a substantially increased accuracy. SPV measurements performed on a-Si_xC_{1-x}:H passivated p- and *n*-type silicon wafers demonstrate the amphoteric behaviour of the fixed charge density at the a-SiC/c-Si interface. This outcome is supported by the qualitative modelling of the extracted S_{eff} data using a simple SRH surface model. The results indicate, that the predominant passivation mechanism of Si-rich a-Si_xC_{1-x}:H is not the field-effect, but a very effective saturation of interface dangling bonds.

8 ACKNOWLEDGMENTS

The authors would like to thank T. Kalden and S. Soebijantoro for the grinding of the wafers and N. Wilhelm for the QSS-PL measurements.

Thomas Roth gratefully acknowledges a scholarship of the German Federal Environmental Foundation (Deutsche Bundesstiftung Umwelt).

This work was supported by the Federal Ministry for Environment, Nature Conservation and Nuclear Safety (BMU) under contract no. 0327610A (SICPASS).

9 REFERENCES

[1] S. Dauwe, L. Mittelstädt, A. Metz and R. Hezel, Progress in Photovoltaics: Research and Applications 10 (2002) 271.

[2] S. Dauwe, J. Schmidt and R. Hezel, Proceedings of the 29th IEEE Photovoltaics Specialists Conference, New Orleans, Louisiana, USA (2002) 1246.

[3] L. Korte, E. Conrad, H. Angermann, R. Stangl and M. Schmidt, Proceedings of the 22nd European Photovoltaic Solar Energy Conference, Milan, Italy (2007) 859.

[4] I. Martín, M. Vetter, A. Orpella, J. Puigdollers, A. Cuevas and R. Alcubilla, Applied Physics Letters 79 (2001) 2199.

[5] S.W. Glunz, S. Janz, M. Hofmann, T. Roth and G. Willeke, Proceedings of the 4th World Conference on Photovoltaic Energy Conversion, Waikoloa, Hawaii, USA (2006) 1016.

[6] R. Ferre, I. Martín, M. Vetter, D. Baetzner, J. Tan, A. Cuevas and R. Alcubilla, Proceedings of the 21st European Photovoltaic Solar Energy Conference, Dresden, Germany (2006) 919.

[7] H. Kampwerth, S. Rein and S.W. Glunz, Proceedings of the 3rd World Conference on Photovoltaic Energy Conversion, Osaka, Japan (2003) 1073.

[8] R.A. Sinton, A. Cuevas and M. Stuckings, Proceedings of the 25th IEEE Photovoltaic Specialists Conference, Washington DC, USA (1996) 457.
[9] T. Trupke, R.A. Bardos, F. Hudert, P. Würfel, J. Zhao, A. Wang and M.A. Green, Proceedings of the 19th European Photovoltaic Solar Energy Conference, Paris, France (2004) 758.
[10] T. Roth, M. Rüdiger, P. Rosenits, S. Diez, T. Trupke, R.A. Bardos and S.W. Glunz, Proceedings of the 22nd European Photovoltaic Solar Energy Conference, Milan, Italy (2007) 1002.
[11] T. Trupke, R.A. Bardos and M.D. Abbott, Applied Physics Letters 87 (2005) 184102.
[12] M.J. Kerr and A. Cuevas, Journal of Applied Physics 91 (2002) 2473.
[13] H.Schlangenotto, W.Gerlach, Phys. Status Solidi A 21 (1974) 357.
[14] A.B. Sproul, Journal of Applied Physics 76 (1994) 2851.
[15] R.B.M. Girisch, R.P. Mertens and R.F. De Keersmaecker, IEEE Transactions on Electron Devices 35 (1988) 203.
[16] S.W. Glunz, D. Biro, S. Rein and W. Warta, Journal of Applied Physics 86 (1999) 683.
[17] Y.W. Lam, J. Phys. D: Appl. Phys. 4 (1971) 1370; A. Laades, PhD Thesis, Technische Universität Berlin, 2005.
[18] I. Martín, Silicon surface passivation by Plasma Enhanced Chemical Vapor Deposited amorphous silicon carbide films, PhD Thesis, Polytechnical University of Catalonia, Spain, 2004.
[19] S. Olibet, E. Vallat-Sauvain and C. Ballif, Physical Review B 76 (2007) 035326.
[20] S. Dauwe, Low-temperature surface passivation of crystalline silicon and its application to the rear side of solar cells, PhD Thesis, Universität Hannover, Hannover, 2004.